

# Generic Contrast Agents

Our portfolio is growing to serve you better. Now you have a *choice*.



[VIEW CATALOG](#)

# AJNR

## MR Imaging of Muscles of Mastication

Kurt P. Schellhas

*AJNR Am J Neuroradiol* 1989, 10 (4) 829-837  
<http://www.ajnr.org/content/10/4/829>

This information is current as  
of May 30, 2025.

## MR Imaging of Muscles of Mastication

Kurt P. Schellhas<sup>1</sup>

High-field MR imaging was used to study structural and physiologic alterations involving the muscles of mastication in 46 patients. Muscular abnormalities were often detected incidentally in conjunction with lesions of the CNS, cranial nerves, facial bones, and/or temporomandibular joint (TMJ). Specific pathologic alterations observed included anomalies of musculoskeletal development, muscle hypertrophy, atrophy (disuse and denervation), inflammatory disorders, injuries (including contusions, tears, and muscle rupture), posttraumatic musculoskeletal deformities, and reflex sympathetic dystrophy. Atrophy, fatty replacement, fibrosis, and contracture of selected muscles of mastication may accompany internal derangement of the TMJ in the absence of traumatic deformity.

We conclude that MR is a highly accurate imaging method for detecting masticatory muscle disease. Nontraumatic anatomic and physiologic abnormalities of the muscles of mastication are uncommon disorders. Demonstrable muscle alterations frequently accompany fracture dislocations of the mandibular condyle neck and related facial bones onto which masticatory muscles attach.

Imaging of the trigeminal nerve and TMJ has been revolutionized by thin-section CT and MR [1–15]. The normal and abnormal muscles of mastication and cranio-mandibular apparatus may be routinely studied with head- and surface-coil MR imaging techniques. We investigated the MR characteristics of various structural and physiologic alterations within the muscles of mastication by using high-field MR imaging.

### Materials and Methods

We selected for retrospective study 46 patients (14–69 years old) in whom abnormalities of the muscles of mastication were demonstrated with high-field MR imaging. Cases of radiologically demonstrable muscle abnormalities were selected from over 2600 surface-coil studies of the temporomandibular joint (TMJ) (over 1500 patients) and 1400 MR studies of the brain, head, salivary glands, and facial region (over 2800 total patients) obtained at an outpatient imaging center during a 28-month period. All cases in the study were either formally interpreted or reviewed by a single investigator. At least 100 patients had both surface-coil MR studies of the TMJ and head-coil studies of the brain, masticatory muscles, and face. In many cases, masticatory muscle abnormalities were observed incidentally during evaluation of the brain, head, and neck; however, muscle disease was prospectively considered in all patients, especially those with a history of mandible-facial trauma and those having surface-coil TMJ imaging [8, 10–12].

Indications for brain-head imaging studies (performed with the head coil) where muscle lesions were found incidentally were diverse and included headache; facial pain; otalgia; decreased hearing; cranial nerve deficits; recent head and/or facial injury; suspicion of demyelinating disease; and question of CNS, skull base, temporal bone, salivary gland, or paranasal sinus neoplasia and/or inflammatory disease.

Indications for TMJ surface-coil studies included headache; TMJ and/or ipsilateral facial pain; otalgia; decreased hearing; TMJ clicking; crepitus and/or locking; asymmetric jaw movement during either speech or mastication; recent TMJ and/or mandibular injury; facial

This article appears in the July/August 1989 issue of *AJNR* and the October 1989 issue of *AJR*.

Received September 7, 1988; revision requested November 1, 1988; revision received December 5, 1988; accepted December 6, 1988.

Presented in part at the annual meeting of the Society for Magnetic Resonance Imaging, Boston, March 1988.

Presented at the annual meeting of the American Society of Neuroradiology, Chicago, May 1988.

<sup>1</sup> Center for Diagnostic Imaging, 5775 Wayzata Blvd., Suite 190, St. Louis Park, MN 55416. Address reprint requests to K. P. Schellhas.

*AJNR* 10:829–837, July/August 1989

©195–6108/89/1004–0829

© American Society of Neuroradiology

asymmetry, where muscle pathology was a major consideration; and recent change in skeletal occlusion within 12 months of imaging. Most patients who underwent MR study of the TMJ had been screened with submentovertex and anteroposterior, jaw-protruded radiographs and tightly collimated closed- and open-mouth lateral TMJ tomograms to assess osseous structures.

Three normal volunteers (22–38 years old) underwent both head and TMJ MR studies for the purpose of providing normal muscle images (Figs. 1 and 2). In addition, a normal 61-year-old woman had surface-coil TMJ imaging to assess muscle size and morphology (Fig. 3). The masticatory muscles were carefully studied in normal volunteers and compared with cases of suspected abnormality. Side-to-side symmetry in muscle size, length, and intrinsic signal characteristics was assessed in each patient. Care was taken to clearly identify each muscle within each patient and compare cases of suspected abnormality with relatively age-matched ( $\pm 5$  years) normal individuals when normal controls were available.

All studies were performed with a 1.5-T superconducting G.E. magnet. Each head study was performed with a commercially available head coil and tailored toward the specific anatomy and complaints in question. A typical study of the brain, trigeminal ganglia, and masticatory muscles included a sagittal, 5-mm-thick MR image, 500–600/20/1, 2 (TR range/TE/excitations) with a  $256 \times 128$  matrix and a 24-cm field of view (FOV), followed by multiecho axial (2000–3200/30, 80–100/1, 2) and coronal (600–900/20/1) or multiecho (2400–2800/30, 800–100/1, 2) 3–5-mm-thick images with 1–2.5-mm interspaces, respectively, between images.

Surface-coil studies of the TMJ were performed with either a single, commercially available 8.9-cm round, receive-only surface coil or a dual 8.9-cm round, bilateral, receive-only surface-coil apparatus, with coupled coils designed to prevent radiofrequency feedback. A typical screening TMJ study employed a preliminary axial, 300–600/20/1, sequence with three to eight 5-mm-thick images obtained for mandibular condyle localization and morphology, followed by seven to nine nonorthogonal, 3-mm-thick images (500–2500/20–25, 80–100/1, 2) with a 1-mm interspace,  $256 \times 192$ – $256$  matrix, and 12–13-cm FOV through the full width of each condyle, scanning perpendicular

to the long condylar axis. Short GRASS (gradient-recalled acquisition in the steady state) scans were routinely performed with the mouth closed, partially open, and fully open after closed-mouth multiecho long TR/short and long TE pulse sequences. Further details of surface-coil single- and dual-coil TMJ studies have been previously described [8, 11–15].

## Results

Eight patients exhibited anomalous craniomandibular development such as acquired, nontraumatic facial asymmetry with either enlarged (hypertrophic) (Figs. 4 and 5) or small (hypoplastic-atrophic) (Fig. 6) muscles of mastication either unilaterally or bilaterally (Table 1). We observed either old or recent traumatic injuries affecting the muscles of mastication in 18 patients; these injuries included muscle laceration, contusion, rupture, alteration in length, fibrosis, and focal tears (Figs. 7–9). Two patients exhibited findings compatible with reflex sympathetic dystrophy (RSD) involving the entire unilateral masticatory musculature in conjunction with a history of previous trauma, including skull fracture requiring craniotomy (Fig. 10) and fracture dislocation of the mandibular condyle neck (Fig. 11). Five patients with diffuse masticatory muscle atrophy had an underlying systemic illness such as myasthenia gravis (Fig. 12), polymyositis, progressive systemic sclerosis, or rheumatoid arthritis (Fig. 13). Three patients had unilateral muscle atrophy associated with mass lesions arising either within or adjacent to and externally compressing the ipsilateral trigeminal ganglion (Fig. 14). Nine patients exhibited such findings as muscle hypoplasia, atrophy, and/or fatty replacement of the superior belly of the lateral pterygoid muscle (SBLP) in conjunction with internal derangements of the TMJ (Figs. 15–19). One patient with a 3-month history of severe TMJ pain and a documented (with

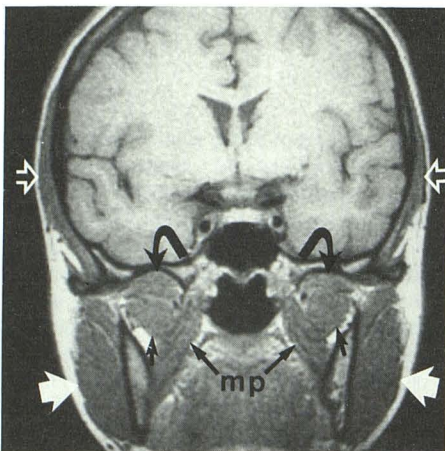


Fig. 1.—Normal muscles of mastication in 32-year-old female volunteer with medium build. Closed-mouth coronal 3-mm-thick MR image, 800/20, with head coil shows normal temporalis (open arrows), masseters (solid white arrows), and medial pterygoids (mp), representing the muscles of jaw closure. Superior (curved arrows) and inferior (small black arrows) bellies of lateral pterygoids function in mouth opening.

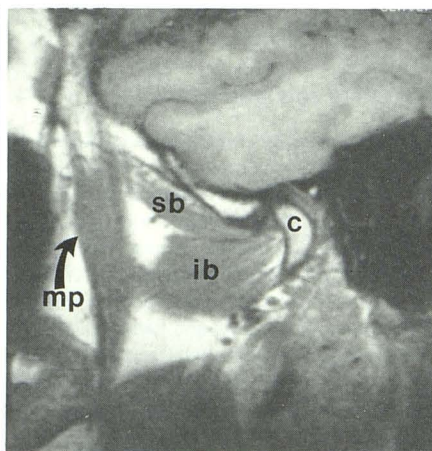


Fig. 2.—Normal pterygoid muscles and TMJ in 37-year-old male volunteer with average build. Sagittal, 3-mm-thick MR image, 500/20, with surface coil (with mouth closed in centric occlusion) reveals normal superior (sb) and inferior (ib) bellies of lateral pterygoids. mp = medial pterygoid, c = mandibular condyle.

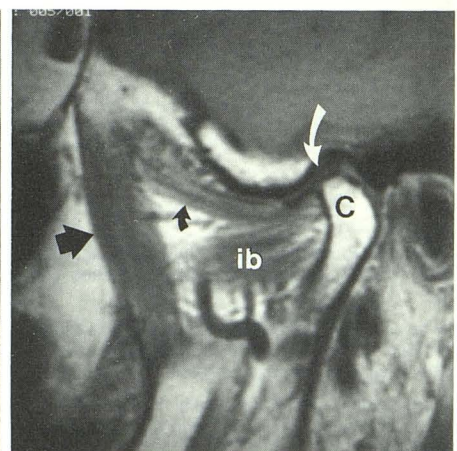
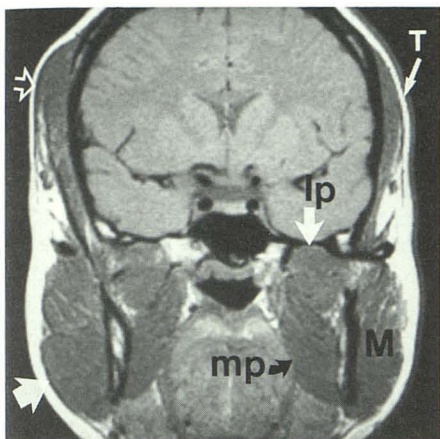
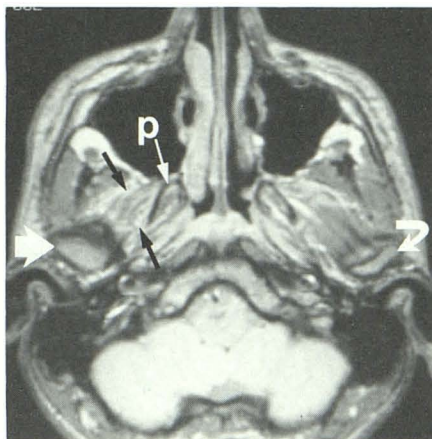


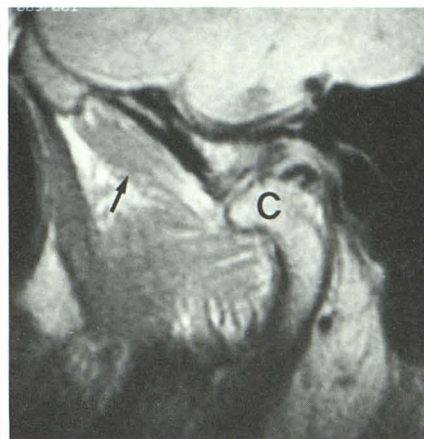
Fig. 3.—Normal pterygoids and TMJ in 61-year-old female volunteer with average build. Sagittal MR image, 600/20, with mouth closed, shows normal medial (large black arrow) pterygoid. Superior (curved black arrow) and inferior (ib) bellies of lateral pterygoids control TMJ meniscus (curved white arrow) and mandibular condyle (c), respectively.



**Fig. 4.**—Hypertrophic muscles of mastication in 24-year-old woman with right-sided temporal headaches, tender temporalis muscles, and long history of nocturnal bruxism. Coronal, 3-mm-thick MR image, 800/20, reveals asymmetric hypertrophy between left- and right-sided temporalis (T), masseter (M), lateral (lp), and medial pterygoid (mp) muscles. Note massively hypertrophic right temporalis (*open arrow*) and masseter (*solid arrow*) compared with moderately hypertrophic left side (compare with Fig. 1).



**A**

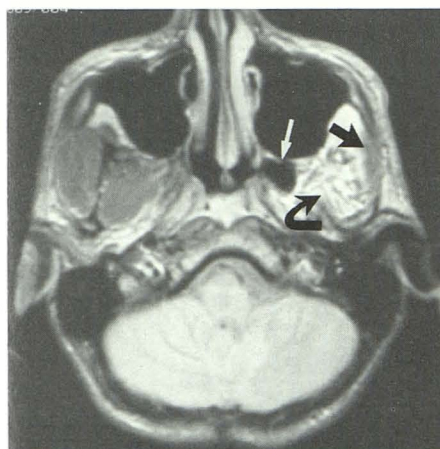


**B**

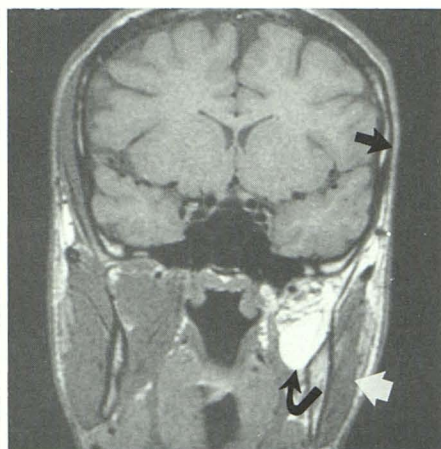
**Fig. 5.**—Asymmetric lateral pterygoid muscle length resulting from developmentally hypertrophic mandibular condyle in 32-year-old man with long history of right-sided headache, facial pain, and TMJ dysfunction.

**A,** Axial MR image, 2000/30, shows enlarged right condyle (*large white arrow*) with shortened superior belly of right lateral pterygoid muscle (*black arrows*). *Curved arrow* = normal left condyle, *p* = normal right pterygoid plate.

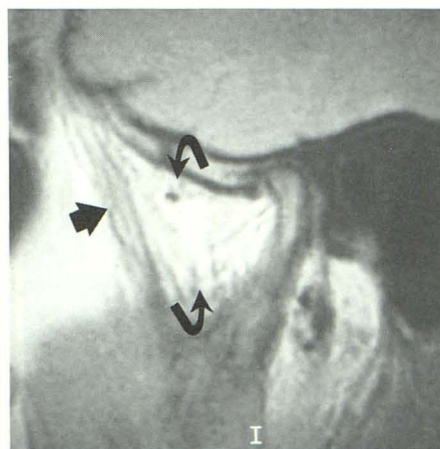
**B,** Closed-mouth sagittal TMJ MR image, 600/20, shows enlarged and deformed condyle (C) with shortened superior belly of right lateral pterygoid (*arrow*).



**A**



**B**



**C**

**Fig. 6.**—Severe developmental masticatory muscle atrophy and contracture in 17-year-old boy with asymmetric jaw motion and severely restricted left condylar motion resulting from childhood facial injury. Coronoid process (not shown) is severely hypoplastic.

**A,** Axial, 5-mm-thick MR image, 2400/30, shows fatty replacement of pterygoids (*curved arrow*) and atrophy of masseter (*straight black arrow*). Note asymmetrically enlarged and aerated left pterygoid plate (*white arrow*).

**B,** Coronal, 3-mm-thick MR image, 800/20, shows complete fatty replacement and fibrosis of temporalis (*straight black arrow*) and pterygoids (*curved arrow*). Left masseter (*white arrow*) is atrophic but less involved than temporalis and pterygoids. Right-sided muscles slightly hypertrophic (compare with Figs. 1 and 4).

**C,** Closed-mouth sagittal TMJ MR image, 700/20, with surface coil reveals severe atrophy and fatty replacement of medial (*straight arrow*) and lateral (*curved arrows*) pterygoids.

MR imaging) inflammatory TMJ arthropathy exhibited ipsilateral atrophy of the entire masticatory musculature, suggesting pain-induced RSD. Fascial-space fluid was observed above and surrounding the SBLP in association with inflammatory TMJ arthropathy and large upper-joint-compartment effusions (Fig. 20) [15].

**Discussion**

The major muscles of mastication receive motor innervation from the mandibular division (V-3) of the trigeminal nerve. The larger jaw-closure muscles include the medial pterygoid, temporalis, and masseter. Muscles of jaw opening include the

superior and inferior belly of the lateral pterygoid, innervated by V-3, and the platysma and anterior belly of the digastric, both of which receive motor supply from the 7th cranial nerve. Normal and hypertrophic masticatory muscles are usually well visualized with both head- and surface-coil MR studies, appearing mildly hypointense and of uniform intrinsic signal intensity with either T1-weighted or long TR/short TE images (Figs. 1–4, 19) [2, 7, 8, 11]. Tendons are well delineated by their very low intrinsic signal, which contrasts sharply with adjacent muscle and fat. Side-to-side symmetry of muscle size, morphology, and intrinsic signal characteristics within

**TABLE 1: Diagnoses Associated with MR Alterations in the Muscles of Mastication (n = 46, ages = 14–69 years)**

| Diagnosis                                                                   | Number of Patients |
|-----------------------------------------------------------------------------|--------------------|
| Anomalous development                                                       | 8                  |
| Trauma                                                                      |                    |
| Old                                                                         | 10                 |
| Recent                                                                      | 8                  |
| Posttraumatic reflex sympathetic dystrophy                                  | 2                  |
| Systemic illness                                                            |                    |
| Myasthenia gravis                                                           | 1                  |
| Polymyositis                                                                | 1                  |
| Progressive systemic sclerosis                                              | 1                  |
| Rheumatoid arthritis                                                        | 2                  |
| Mass lesion affecting trigeminal ganglion                                   | 3                  |
| Internal derangement of TMJ (no associated fracture of traumatic deformity) | 9                  |
| Reflex sympathetic dystrophy accompanying inflammatory TMJ arthropathy      | 1                  |
| Total                                                                       | 46                 |

each individual is most important, since marked variation between patients is the rule. Variations between individuals relate to a broad range of factors, including skeletal size (genetic and/or growth related), age, masticatory habits, and general health (Figs. 1–6, 12, 13). Factors that might influence masticatory muscle appearance should be sought in patients exhibiting muscle abnormalities on MR studies.

Normal and abnormal masticatory muscles may be studied with sequential MR images during various stages of the masticatory cycle with either T1-weighted or GRASS fast scans to simulate dynamic muscle function (Fig. 9) [8, 9, 11, 12]. Anomalous musculoskeletal development, such as either facial or mandibular hemihypertrophy/hemiatrophy may result in demonstrable asymmetry in masticatory muscle size and length (Figs. 5 and 6). Alterations of muscle length and/or mass may result in a decreased force (amplitude) and length (distance) of contraction, which might secondarily affect mastication and/or phonation by causing asymmetric jaw motion and function. Internal derangements of the TMJ may cause similar clinical afflictions by interfering with normal joint and masticatory muscle function.

Atrophic muscles on occasion exhibit increased signal on short and long TR/short TE images due to dystrophic changes and/or fatty replacement (Figs. 6, 8, 10–15). Familial masticatory muscle hypertrophy has been described [16, 17]. Mandibular coronoid process hypertrophy is known to result in chronic restriction of TMJ mobility, in many instances leading to atrophy and contracture of the muscles of jaw closure due to decreased range of motion and the lack of periodic muscle stretching [18].

Atrophy, fatty replacement, and fibrosis of the muscles of mastication occur with either disuse or denervation. Disuse atrophy is frequently observed after immobilization, in debili-

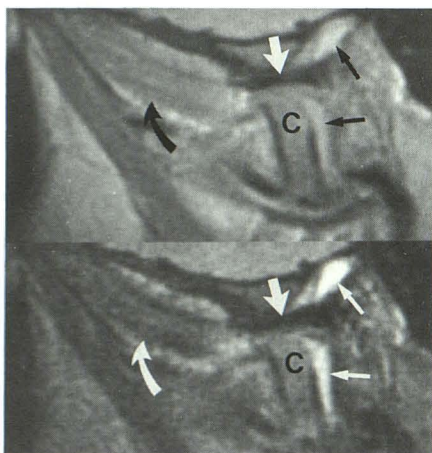


**Fig. 7.**—Lateral pterygoid muscle shortening 3 weeks after fracture dislocation of mandibular condyle (C) in 14-year-old boy. Closed-mouth sagittal TMJ MR images, 2200/25 (top) and 2200/80 (bottom), reveal shortening of superior belly of right lateral pterygoid (curved arrows). TMJ meniscus (large white arrows) remains normally positioned relative to condyle, separating upper- and lower-joint-compartment fluid collections (small arrows).

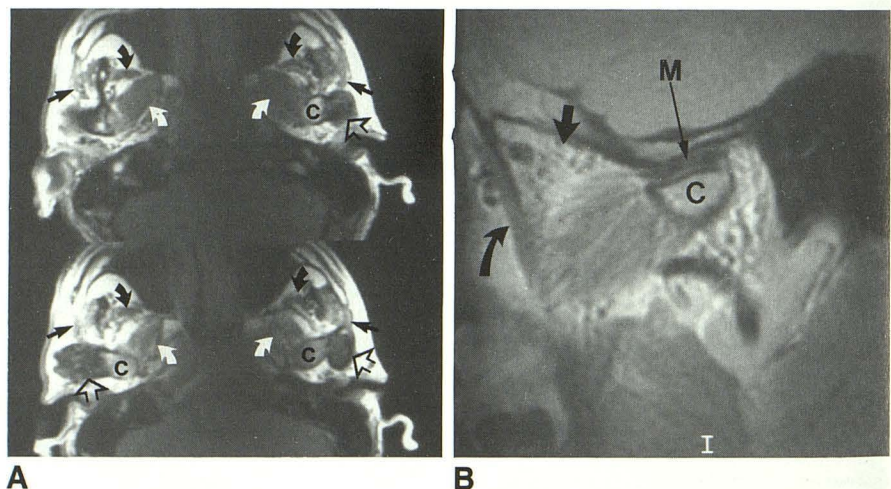


**Fig. 8.**—Severe muscle atrophy and contracture resulting from old, healed bilateral condylar neck fracture dislocations in 44-year-old man with only 4 mm of vertical mouth opening.

**A,** Axial, 5-mm-thick, adjacent MR images, 500/20, obtained with dual TMJ surface-coil apparatus, show displaced condyles (C) with large calluses (open arrows) originating from healed condylar neck fractures. Medial pterygoids (curved black arrows) and masseters (solid black arrows) are severely atrophic.

**B,** Closed-mouth, sagittal, 3-mm-thick, surface-coil MR image, 2200/25, of left TMJ reveals atrophic medial pterygoid (curved arrow) with severe fibrosis of superior belly of right lateral pterygoid (straight arrow). (Compare with lower image in A.) TMJ meniscus (M) is normally positioned relative to deformed mandibular condyle (C).

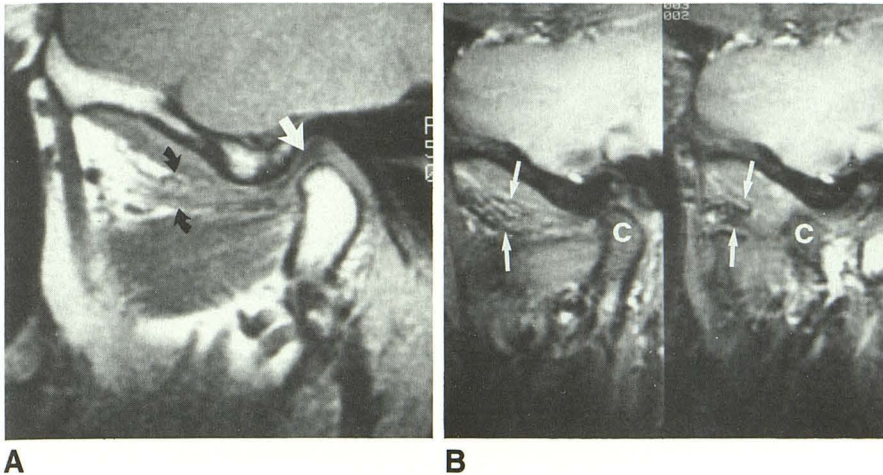


**Fig. 9.**—Partial muscle tear in 56-year-old woman who experienced severe TMJ and facial pain after posterior molar extractions performed under general anesthesia.

**A,** Sagittal, closed-mouth MR image, 600/20, shows partial tear and retraction of inferior fibers (curved black arrows) of superior belly of right lateral pterygoid (compare with Figs. 2, 3, and 5). TMJ meniscus (white arrow) is normal in position and morphology.

**B,** Closed- (left) and open-mouth (right) sagittal GRASS images show nonfunction of torn muscle fibers (arrows) during mouth opening. C = mandibular condyle.

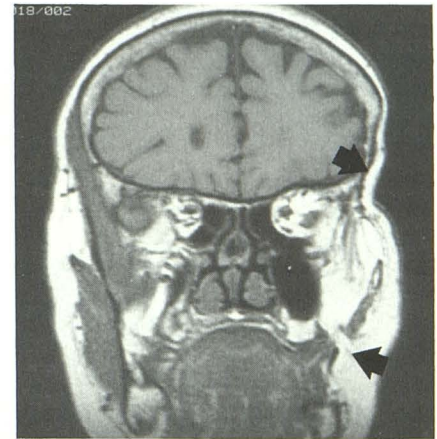


**Fig. 10.**—Severe muscle atrophy suggesting posttraumatic reflex sympathetic dystrophy in 65-year-old woman with severe left-sided headache, facial pain, and restricted jaw motion 20 years after left-sided skull fracture and craniotomy. Coronal, 3-mm-thick MR image shows complete fatty replacement of masticatory muscles (arrows). Opposite side is normal for age.

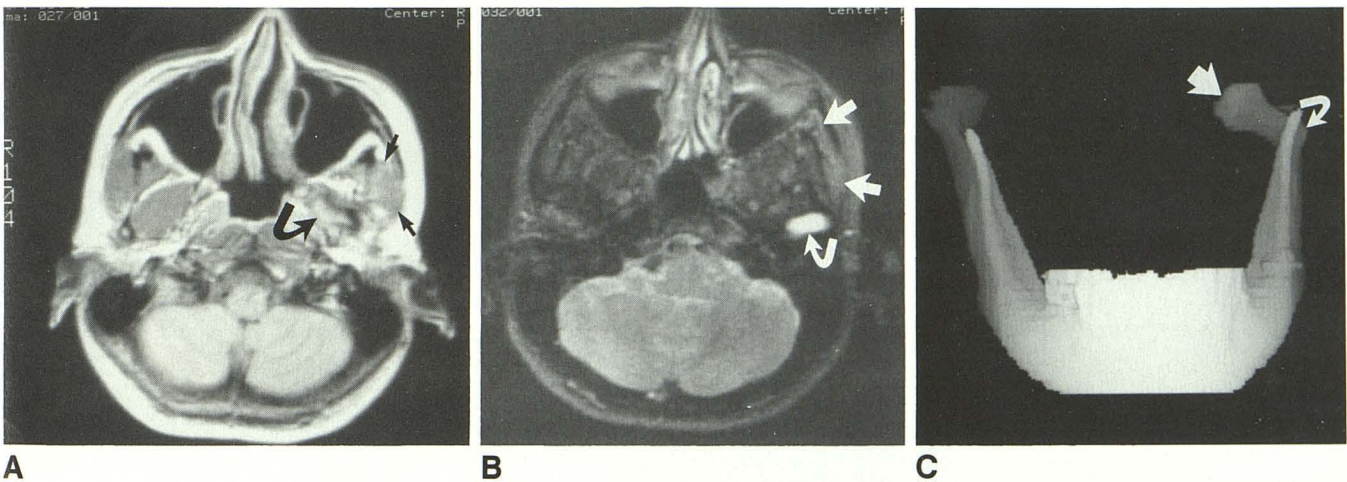


**Fig. 11.**—Posttraumatic reflex sympathetic dystrophy 3 months after fracture dislocation of mandibular condyle in 46-year-old woman with severe, constant left-sided facial pain, unilateral muscle wasting, and complete loss of mouth-opening ability.

**A,** Axial, 5-mm-thick MR image, 2000/20, shows dislocated condyle (curved arrow) with normal intrinsic marrow signal. Masseter (straight arrows) exhibits higher signal than opposite side. (Reprinted with permission from [10].)

**B,** Axial MR image, 2000/80, above that in A, reveals signal-intense fluid (curved arrow) within empty glenoid fossa and slightly increased signal within clinically atrophic and tender left masseter (straight arrows).

**C,** Frontal view of three-dimensional CT scan of disarticulated mandible shows displaced condyle (straight arrow) and callus (curved arrow) at site of healed condylar neck fracture. Severe pain, muscle wasting, and avascular necrosis of left mandibular condyle was noted 18 months after MR imaging. Patient has refused follow-up MR study because of claustrophobia. Avascular necrosis was diagnosed with radiography and tomography.

tating diseases, and with advanced age [19]. Muscle fibrosis and contracture may follow prolonged immobilization and disuse. Denervation atrophy may occur with either structural lesions (masses) affecting the brain, trigeminal ganglion (Fig. 14) and/or peripheral trigeminal nerve branches, in generalized inflammatory diseases (Fig. 13), and in cases of biochemical denervation, such as myasthenia gravis (Fig. 12) [1, 20]. Simultaneous fatty replacement and muscle edema may be

observed with multiecho, long TR/short and long TE images during the active phase of muscle resorption following denervation (Fig. 14).

Traumatic injuries to the brain, face, mandible, and TMJ may all affect either the trigeminal neuraxis or the muscles of mastication [8, 10, 14, 15]. Muscle tears, alterations in muscle length, contusions, and tendon ruptures are all demonstrable posttraumatic sequelae. The radiologic diagnosis of both

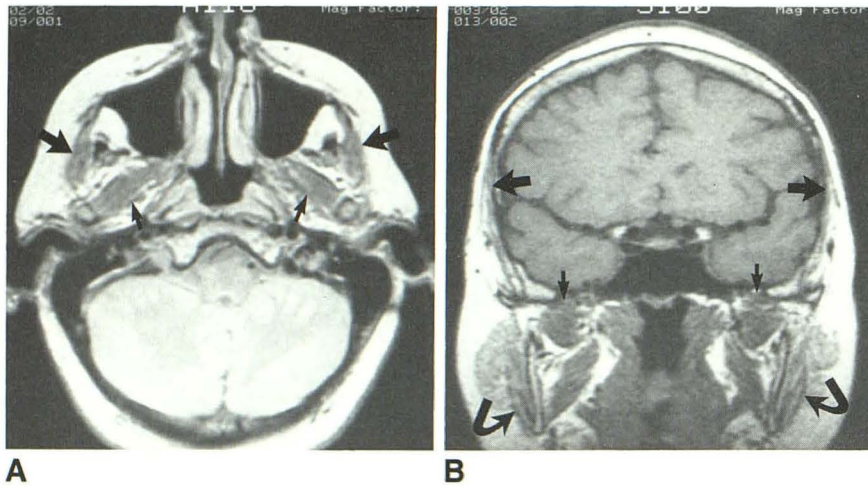


Fig. 12.—A and B, Muscle atrophy caused by myasthenia gravis in 49-year-old woman with masticatory muscle weakness and wasting scanned for suspected brainstem disease. Axial (A), 2000/20, and coronal (B), 800/20, MR images reveal severe atrophy affecting the temporalis (*large straight arrows*) and masseters (*curved arrows*). Lateral pterygoids (*small arrows*) are moderately atrophic. Myasthenia gravis was diagnosed after muscle atrophy was noted and brainstem disease ruled out.

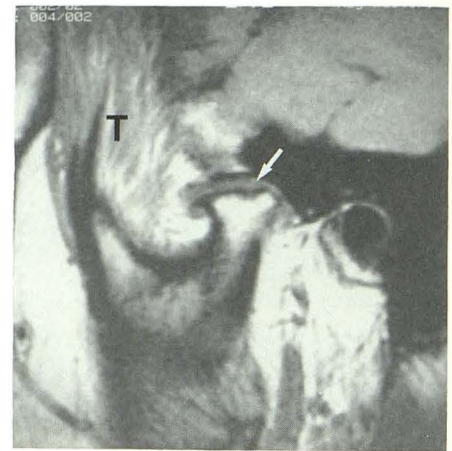


Fig. 13.—Temporalis atrophy and fatty replacement associated with long-standing rheumatoid arthritis and painful, degenerated TMJ. Sagittal, closed-mouth MR image, 600/20, reveals increased fat within temporalis (T) muscle. Note absence of meniscus from fluid-filled joint compartment (*arrow*) and flattening of mandibular condyle. Meniscus (not seen) was dislocated anteromedially on more medial images.

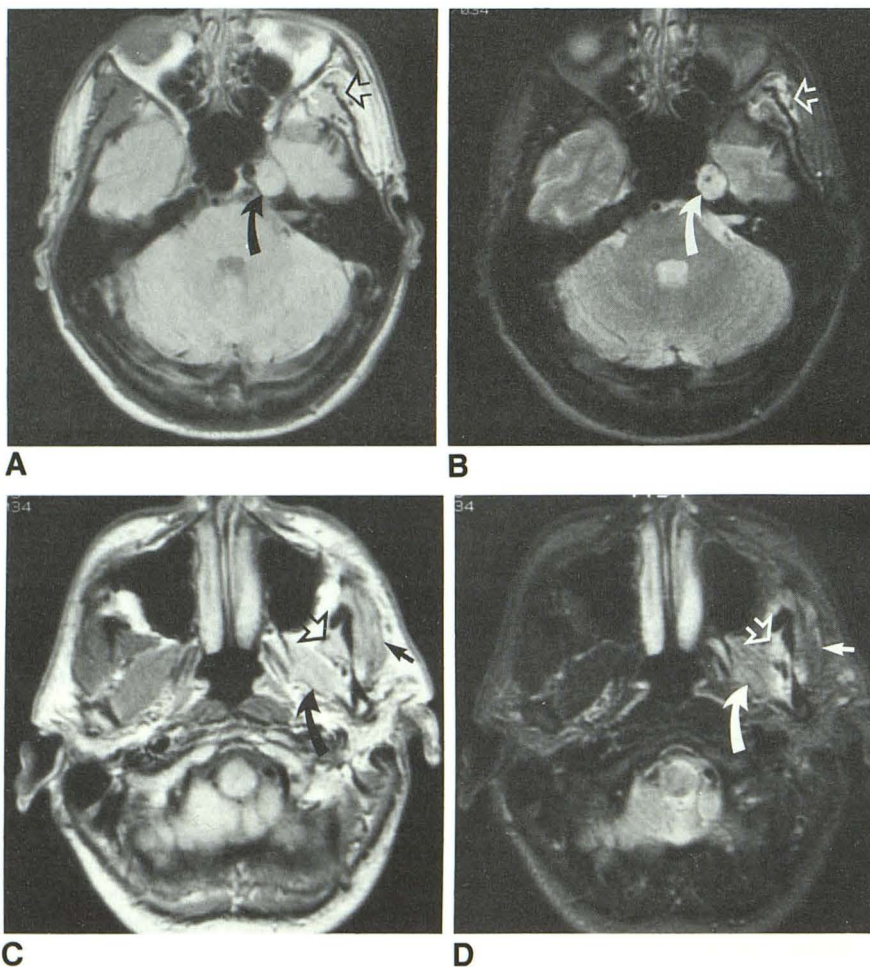


Fig. 14.—Subacute denervation atrophy caused by surgically confirmed schwannoma of the trigeminal ganglion in 31-year-old man with progressive, unilateral jaw weakness and externally visible muscle wasting of 3–5 months duration.

A and B, Axial MR images, 2000/20 (A) and 2000/80 (B), reveal mass (*curved arrows*) within Meckel's cave. Muscle atrophy and increased signal (*open arrows*) are thought to reflect fatty replacement and cellular–extracellular inflammation and edema.

C and D, Masseter (*small straight arrows*), temporalis (*open arrows*), and lateral pterygoid (*curved arrows*) exhibit fatty replacement and increased fluid caused by proximal denervation.

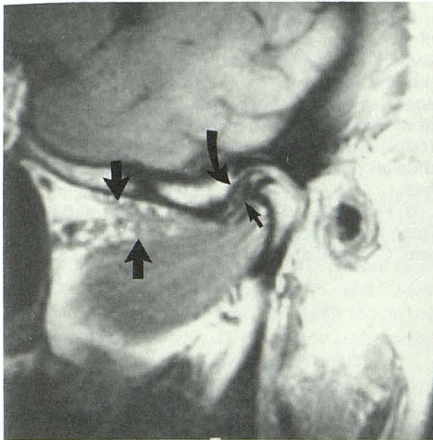
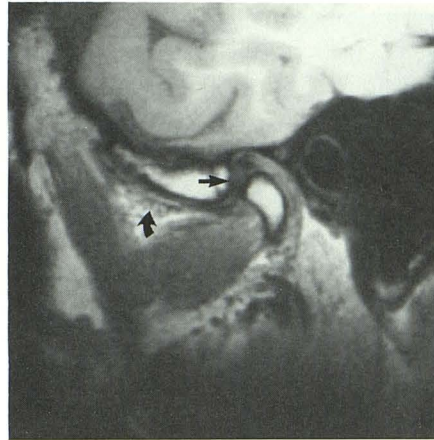
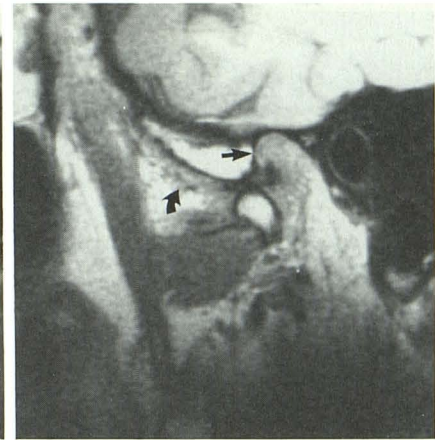


Fig. 15.—Atrophy and fatty replacement of superior belly of right lateral pterygoid in 24-year-old man with chronic TMJ pain and dysfunction. Superior belly of right lateral pterygoid (*large straight arrows*) is atrophic. TMJ meniscus (*small straight arrow*) is anteriorly displaced. Glenoid fossa articular surface (*curved arrow*) is nearly vertical. Mechanical joint symptoms and pain resolved completely after meniscectomy.



A



B

Fig. 16.—A and B, Developmental muscular hypoplasia versus acquired atrophy and fibrosis of superior belly of right lateral pterygoid associated with unusually deep glenoid fossa configuration in 24-year-old woman with TMJ clicking, facial pain, and episodic joint locking. Closed- (A) and open-mouth (B) sagittal TMJ MR images, 600/20, reveal a deep glenoid fossa and steep articular eminence (*straight arrows*). Superior belly of right lateral pterygoid (*curved arrows*) is small and either severely underdeveloped or atrophic.

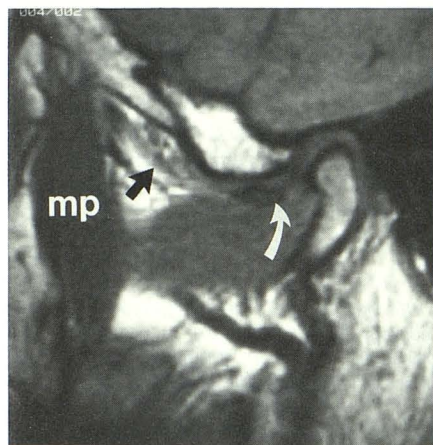


Fig. 17.—Atrophy, fibrosis, and contracture of superior belly of right lateral pterygoid associated with chronic displacement of TMJ meniscus. Sagittal, closed-mouth TMJ MR image, 600/20, reveals atrophy and fibrosis of superior belly of right lateral pterygoid (*straight arrow*) with anterior displacement, thickening, and deformity of TMJ meniscus (*curved arrow*). Adjacent medial pterygoid (mp) muscle is normal.

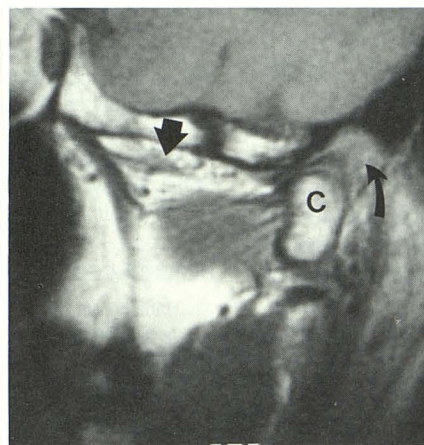


Fig. 18.—Atrophy, fibrosis, and contracture of superior belly of right lateral pterygoid (*straight arrow*) after 4 years of TMJ therapy with progressive, anterior-repositioning intraoral splints in 39-year-old woman with long history of TMJ pain and worsening malocclusion during treatment. No pretreatment imaging. Sagittal, closed-mouth MR image, 600/20, without splint shows widened space (*curved arrow*) behind condyle (C). Note normal meniscus and anterior position of condyle due to iatrogenic occlusal changes (compare with Figs. 2, 3, and 17).

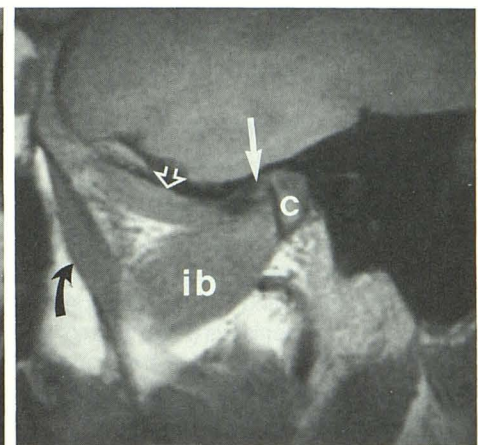


Fig. 19.—Normal pterygoid muscles with anterior displacement of TMJ meniscus. Closed-mouth sagittal MR image through medial pole of mandibular condyle (c) reveals anteromedial displacement of meniscus (*white arrow*) with normal pterygoid muscles. *Open arrow* = superior belly of right lateral pterygoid, *ib* = normal inferior belly of lateral pterygoid, *curved arrow* = normal medial pterygoid.

acute and chronic traumatic muscle alterations is important, since changes in muscle function often occur after muscle tear, shortening, and/or rupture (Figs. 7–9). Muscle injuries and alterations in muscle length that result from fracture dislocations of the mandible may result in significant disability (Figs. 8–11). Localized edema and fascial-space inflammation

may accompany contusions, direct muscle injuries, and TMJ inflammation (Fig. 20). We have observed muscle tears after pharyngeal surgery and posterior dental extractions due to overdistraction and/or excessive lateral mobilization of the jaw under general anesthesia (Fig. 9). RSD of the masticator muscles is a poorly understood posttraumatic sequela of

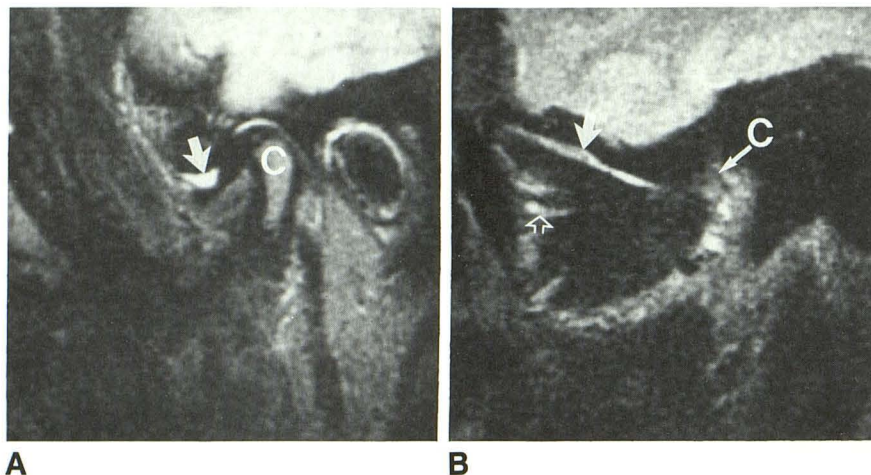


Fig. 20.—Fascial-space edema caused by non-infectious, inflammatory TMJ arthropathy in adult woman with recent onset of facial/TMJ pain, otalgia, and ipsilateral open bite. Closed-mouth, adjacent, sagittal MR images, 2500/100, through center of condyle (A) and medial pole of condyle (B).

A, Large, signal-intense, upper-compartment effusion (arrow) is present. C = mandibular condyle.

B, Fluid is seen above (solid arrow) and below (open arrow) superior belly of right lateral pterygoid. C = medial pole of condyle.

craniomandibular injury that results in pain, muscle wasting, skeletal demineralization, and disability as it does in the appendicular skeleton (Figs. 10 and 11) [21–24].

It is theorized that RSD results from excessive sympathetic stimulation and/or parasympathetic nonfunction causing vasoconstriction and ischemia in the affected anatomic region, leading to pain and dystrophic changes such as muscle atrophy and skeletal demineralization. RSD often follows either peripheral nerve or nerve plexus injury in the extremities, where it is observed by neurologists, orthopedists, and rehabilitation specialists. The exact frequency of RSD is not known.

Anomalous development, atrophy, fibrosis, and muscle contracture are all observed in conjunction with internal derangements of the TMJ (Figs. 15–18) [4–8, 11, 18, 25]. Hypoplasia versus acquired atrophy of the SBLP muscle is a commonly observed but poorly understood finding associated with unusually deep glenoid fossa configurations, with or without accompanying internal derangement and/or displacement of the TMJ meniscus (Figs. 15 and 16). Atrophy, fibrosis, and contracture of the SBLP are found in selected cases of meniscus derangement and anterior displacement, although this finding is not constant and merits further investigation (Figs. 17–19) [7, 8, 11, 25]. We have noted SBLP fibrosis and contracture associated with the prolonged use of anterior-repositioning intraoral splints used for treatment of TMJ afflictions (Fig. 18). Fascial-space edema surrounding the pterygoid musculature is observed with inflammatory TMJ arthropathy, as intraarticular fluid from the superior joint compartment drains anteromedially toward the pterygopalatine fossa, within and around distended lymphatics, above and between the lateral pterygoids (Fig. 20). This drainage pathway for upper-joint-compartment fluid (or contrast material) has been observed commonly during two-compartment TMJ arthrography with inadvertent rupture of the superior compartment capsule [11]. Atrophy, contracture, and disability of masticatory muscles may occur as sequelae of chronic TMJ and/or facial pain, without history of trauma, suggesting the existence of pain-induced reflex sympathetic dystrophy [22, 24].

In conclusion, structural and physiologic lesions involving the muscles of mastication may be observed with MR imaging

in association with a variety of head and neck disorders. Masticatory muscle abnormalities are most often observed with trauma and less often with anomalous development and internal derangements of the TMJ. The recognition of muscle alterations may lead to a correct diagnosis and improved understanding of the clinical symptomatology and disease pathophysiology under investigation.

#### ACKNOWLEDGMENTS

Thanks to Mark R. Omlie, C. Randall Nelms, Elizabeth A. Reid, James C. Block, Robert J. Keck, John J. Norton, and Eric L. Schiffman for individual case contributions. Special thanks to Clyde H. Wilkes for over half of the 46 cases in the series and to Mark A. Piper for his consultation. The contributions of Kenneth B. Heithoff, Hollis M. Fritts, Becky Borgerson, and the technical staff at the Center for Diagnostic Imaging are sincerely appreciated.

#### REFERENCES

- Harnsberger HR, Dillon WP. Major motor atrophic patterns in the face and neck: CT evaluation. *Radiology* 1985;155:665–670
- Daniels DL, Pech P, Pojunas KW, Kilgore DP, Williams AL, Haughton VM. Trigeminal nerve: anatomic correlation with MR imaging. *Radiology* 1986;159:577–583
- Seltzer SE, Wang AM. Modern imaging of the masseter muscle: normal anatomy and pathosis on CT and MRI. *Oral Surg Oral Med Oral Pathol* 1987;63:622–629
- Harms SE, Wilk RM, Wolford LM, et al. The temporomandibular joint: magnetic resonance imaging using surface coils. *Radiology* 1985;157:133–136
- Katzberg RW, Bessette RW, Tallents RH, et al. Normal and abnormal temporomandibular joint: MR imaging with surface coil. *Radiology* 1986;158:183–189
- Schellhas KP, Wilkes CH, Heithoff KB, Omlie MR, Block JC. Temporomandibular joint: diagnosis of internal derangements using magnetic resonance imaging. *Min Med* 1986;69:516–519
- Harms SE, Wilk RM. Magnetic resonance imaging of the temporomandibular joint. *RadioGraphics* 1987;7:521–542
- Schellhas KP, Wilkes CH, Fritts HM, Omlie MR, Heithoff KB, Jahn JA. Temporomandibular joint: MR imaging of internal derangements and post-operative changes. *AJNR* 1987;8:1093–1101, *AJR* 1988;150:381–389
- Burnett KR, Davis CL, Read J. Dynamic display of the temporomandibular joint meniscus using “fast scan” MR imaging. *AJR* 1987;149:959–962
- Schellhas KP, El Deeb M, Wilkes CH, et al. Three dimensional computed tomography in maxillofacial surgical planning. *Arch Otolaryngol Head Neck Surg* 1988;114:438–442
- Schellhas KP, Wilkes CH, Omlie MR, et al. The diagnosis of temporomandibular joint disease: two-compartment arthrography and MR. *AJNR*

- 1988;9:579-588, *AJR* 1988;151:341-350
12. Schellhas KP, Fritts HM, Heithoff KB, Jahn JA, Wilkes CH, Omlie MR. Temporomandibular joint: MR fast scanning. *J Craniomand Pract* 1988; 6:209-216
  13. Schellhas KP, El Deeb M, Wilkes CH, et al. Permanent proplast temporomandibular joint implants: MR imaging of destructive complications. *AJR* 1988;151:731-735
  14. Schellhas KP, Wilkes CH, Fritts HM, Lagrotteria LB, Omlie MR. MR of osteochondritis dissecans and avascular necrosis of the mandibular condyle. *AJNR* 1989;10:3-12, *AJR* 1989;152:551-560
  15. Schellhas KP, Wilkes CH. Temporomandibular joint inflammation: comparison of MR fast scanning with T1- and T2-weighted imaging techniques. *AJNR* 1989;10:589-594, *AJR* 1989;153:(in press)
  16. Gorlin RJ, Pindborg JJ, Cohen MM. *Syndromes of the head and neck*, 2nd ed. New York: McGraw-Hill, 1976:341-343
  17. Martinelli P, Fabbri R, Gabellini AS, Mazzini G, Rasi F. Familial hypertrophy of masticatory muscles. *J Neurol* 1987;164:811-816
  18. Isberg A, Isacson G, Nah K-S. Mandibular coronoid process locking: a prospective study of frequency and association with internal derangement of the temporomandibular joint. *Oral Surg Oral Med Oral Pathol* 1987; 63:275-279
  19. Ramon Y, Samra H, Oberman M. Mandibular condylosis and apertognathia as presenting symptoms in progressive systemic sclerosis (scleroderma). Pattern of mandibular bony lesions and atrophy of masticatory muscles in PSS, presumably caused by affected muscular arteries. *Oral Surg Oral Med Oral Pathol* 1987;63:269-274
  20. Rigamonti D, Spetzler RF, Shetter A, Drayer BP. Magnetic resonance imaging and trigeminal schwannoma. *Surg Neurol* 1987;28:67-70
  21. Markoff M, Farole A. Reflex sympathetic dystrophy syndrome. Case report with a review of the literature. *Oral Surg Oral Med Oral Pathol* 1986;61: 23-28
  22. Jaeger B, Singer E, Kroening R. Reflex sympathetic dystrophy of the face. Report of two cases and a review of the literature. *Arch Neurol* 1986; 43:693-695
  23. Schwartzman RJ, McLellan TL. Reflex sympathetic dystrophy: a review. *Arch Neurol* 1987;44:555-561
  24. Talacko AA, Reade PC. Hemifacial atrophy and temporomandibular pain-dysfunction syndrome. *Int J Oral Maxillofac Surg* 1988;17:224-226
  25. Wilkes CH. Internal derangement of the temporomandibular joint: pathologic variations. *Arch Otolaryngol Head Neck Surg* 1989;115:469-477